Mobile Netw Appl
DOI 10.1007/s11036-008-0107-8

Channel Access Scheme for MIMO-Enabled Ad Hoc Networks with Adaptive Diversity/Multiplexing Gains

Mohammad Z. Siam · Marwan Krunz

Abstract Transmission power control (TPC) is used in wireless networks to improve channel reuse and/or reduce energy consumption. It has been often applied to single-input single-output (SISO) systems, where each node is equipped with a single antenna. Multi-input multi-output (MIMO) systems can improve the throughput or the signal-to-noise ratio (SNR) by providing multiplexing or diversity gains, respectively. In this paper, we incorporate a power-controlled MAC protocol for a wireless network with two antennas per node. Our protocol, coined CMAC, combines different types of MIMO gains, allowing for dynamic switching between diversity and multiplexing modes so as to maximize a utility function that depends on both energy consumption and throughput. CMAC adapts the "antenna mode," the transmission power, and the modulation order on a per-packet basis. By "antenna mode" we mean one of five possible transmit/receive antenna configurations: 1×1 (SISO), 2×1 (MISO-D), 1×2 (SIMO-D), 2×2 (MIMO-D), and 2×2 (MIMO-M). The second, third, and fourth configurations offer a diversity gain, whereas the last configuration offers a multiplexing gain. By using control packets to *bound* the transmission power of potentially interfering terminals, CMAC allows for multiple interference-limited transmissions to take place in the vicinity of a receiving terminal. We study via simulations the performance of CMAC in ad hoc topologies. Our results indicate that relative to non-adaptive protocols, CMAC achieves a significant improvement in both the overall energy consumption and the throughput.

Keywords power control · ad hoc networks · MIMO · diversity gain · multiplexing gain

This research was supported in part by NSF (under grants CNS-0721935, CNS-0627118, CNS-0325979, and CNS-0313234), Raytheon, and Connection One (an I/UCRC NSF/industry/university consortium). Any opinions, findings, conclusions, or recommendations expressed in this paper are those of the authors and do not necessarily reflect the views of the National Science Foundation. An abridged version of this paper was presented at the *BROADNETS 2007 Conference*, North Carolina, USA, September 10–14, 2007.

M. Z. Siam (✉) · M. Krunz
Department of Electrical and Computer Engineering,
The University of Arizona, Tucson, AZ 85721, USA
e-mail: siam@ece.arizona.edu

M. Krunz
e-mail: krunz@ece.arizona.edu

1 Introduction

1.1 Background

The vast majority of currently deployed wireless local area networks (WLANs) are based on the IEEE 802.11 DCF scheme [1]. Channel access in this scheme is performed according to a variant of carrier sense multiple access with collision avoidance (CSMA/CA) with an optional virtual carrier sensing (VCS) mechanism, i.e., request-to-send/clear-to-send (RTS/CTS) exchange. By default, packets are transmitted at a fixed power level. Several studies demonstrated the inefficiency of the fixed-transmission-power strategy in terms of energy consumption and channel reuse (e.g., [2–4]). Accordingly, several transmission power control (TPC) protocols have been proposed (see [5] for a survey),[1]

[1] Another approach to conserve energy is to put inactive nodes to sleep. Such an approach is complementary to TPC, and is not considered in this paper.

some of which are aimed at energy conservation (e.g., [6–8]) while others are throughput oriented (e.g., [3, 4, 9, 10]). For example, in [8] RTS and CTS packets are transmitted at a maximum power ($P_{\max}$), while data and ACK (acknowledgment) packets are transmitted at the minimum power level that guarantees the required signal-to-noise ratio (SNR). This leads to a reduction in the total energy consumption in the network, but does not improve the channel reuse. The POWMAC protocol [10] addresses the channel reuse issue by redefining the role of the RTS/CTS exchange, making it possible for multiple pairs of neighboring nodes to communicate, provided that the selected power levels do not cause the SNR at any receiver to fall below the required threshold. Other protocols improve the performance by using busy-tones (e.g., [4]) and prioritized back-off (e.g., [11, 12]).

Thus far, much emphasis has been on TPC techniques for single-input single-output (SISO) systems, where each node uses a single antenna for transmission and reception, with the transceiver typically operating in a half-duplex mode. Significant improvement in network performance can be achieved by employing multi-input multi-output (MIMO) techniques [13], whereby multiple transmit and/or receive antennas are exploited to achieve spatial diversity. In principle, MIMO offers three types of gains: *array*, *diversity*, and *multiplexing* [13]. The array gain is achieved either at the transmitter through directional alignment of the transmitted signal or at the receiver through coherent combining of multiple copies of the signal that are received over independent paths. This gain is reflected in an improvement in the received SNR that results from transmitting multiple identical signals over independent paths and *coherently* combining these signals at the receiver. Diversity gain is interpreted as the slope of the average bit error rate (BER) curve versus SNR, which is proportional to the number of independent paths (in the best case, this number is equal to the product $M_t M_r$, where M_t and M_r are, respectively, the numbers of transmit and receive antennas). To realize this gain, space-time coding is used to encode the signal and transmit it over the M_t antennas. Multiplexing gain is obtained when different signals are transmitted over the M_t antennas for the purpose of increasing the total transmission capacity of the link. Note that the diversity and array gains can be used to improve link reliability (i.e., lower the BER), extend the communication distance, or reduce the SNR requirement.

In [14] it was shown that a MIMO-based communication consumes much less *transmission power* than SISO-based communication. Note that this energy saving applies to MIMO with diversity gain, and does not apply for MIMO with multiplexing gain. As a result, the diversity gain results in a better energy performance compared to the SISO mode, whereas the multiplexing gain provides better throughput performance compared to the SISO mode.

As eluded to earlier, for a given target BER, a multi-antenna transmission requires less RF power than a SISO transmission. However, it also requires more circuit power at both ends of the link. As a result, a distance-dependent tradeoff emerges between transmission and circuit powers [15]: for relatively small distances, circuit power is dominant, and hence a SISO mode is more energy-efficient than a multi-antenna mode. As the transmitter-receiver distance increases, the tradeoff shifts in favor of the multi-antenna modes (SIMO, MISO, or MIMO). Joint optimization of transmission/circuit powers was considered in several previous studies (e.g., [15–17]), although the focus was on SISO systems. The authors in [14] proposed a joint energy minimization strategy for a MIMO-based link under a fixed antenna configuration.

The spectral efficiency of a MIMO ad hoc network was studied in [18] with simultaneous communicating transmitter-receiver pairs. In particular, the authors showed that with idealized medium access control, the channelized transmission has unbounded asymptotic spectral efficiency under the constant per-user power constraint. The impact of different power constraints on the asymptotic spectral efficiency was also examined. Various architectures of MIMO systems and their features (including those proposed for the IEEE 802.11n standard) were discussed in [19]. The authors studied the impact on chip area and required data processing rates for MIMO systems. A connectivity metric for MIMO-equipped ad hoc networks was introduced in [20] based on probabilistic analysis of the achievable capacity of random topologies. The authors assumed that pair of nodes are connected if their bi-directional capacity is more than a given threshold. The results showed that employing mobile nodes with multiple antennas enhances the connectivity of fading wireless ad-hoc networks. The authors in [21] formulated the scheduling problem in MIMO-equipped networks as a generalized assignment problem, and provided a cross-layer design for scheduling users and assigning their data to available transmit antennas. The proposed scheduling and antenna sharing method, referred to as fast transmit antenna selection (FTAS), uses adaptive proportional fairness (APF) mapping as a means to determine the user-antenna assignment that maximizes the network performance in terms of both throughput and fairness. The authors in [22] discussed the problem of receive antenna subset selection in MIMO spatial

multiplexing (MIMO-SM) systems. They developed selection algorithms for maximizing the channel capacity. One algorithm in particular allows tractable statistical analysis of performance. The authors leveraged this to prove that the capacity of the system through receive antenna selection is statistically lower bounded by the capacity of a set of parallel independent SIMO channels, each with selection diversity.

1.2 Related work

In [23] the authors characterized the fundamental tradeoffs between the three types of MIMO gains and provided insights on the capabilities of multiple antennas in a networked context. The authors extended the results of a point-to-point wireless fading channel to a multiple-access fading channel. The tradeoff between diversity and multiplexing gains was studied in [24] for three schemes: quasi-orthogonal group space-time (QoGST), group layered space-time (GLST), and layered space-time block codes (LSTBC). A comparison between them demonstrated that QoGST achieves the best diversity-multiplexing tradeoff. The authors in [25] extended the work on the tradeoff function for the MIMO gains (for point-to-point MIMO system when optimal detection is used) to a more general MIMO system, where the transmitted data is coded in groups. In [25], group detection is applied at the receiver to retrieve the data. It consists of a zero-forcing decorrelation that separates the groups, followed by a joint detection for each of the groups. The authors in [25] evaluated the diversity-multiplexing tradeoff for two receiver structures: group zero forcing (GZF) and group successive interference cancellation (GSIC). The author in [26] presented a non-asymptotic framework to analyze the diversity-multiplexing tradeoff of a MIMO wireless system. In addition, exact diversity gain expressions were determined for orthogonal space-time block codes (OSTBC). In [27] the authors considered joint scheduling and beamforming for a broadcast channel with multiple antennas at the transmitter and a single antenna at the mobile receiver, and identified the tradeoff between multi-user diversity and spatial multiplexing gain under a limited amount of feedback. MIR is another protocol that was proposed for MIMO links [28]. Essentially, it is a routing protocol that adapts between the different strategies based on the network conditions. MIR controls the various characteristics of MIMO links (e.g., network density, mobility, link quality) to improve the network performance. Referring to the spatial-multiplexing strategy as MUX, diversity with reduced BER as DIV-BER, and diversity with increased communication range as DIV-RANGE, it was shown that while MUX is the appropriate strategy for dense networks, DIV-RANGE is preferable for sparse networks, where it might not be possible to obtain routes with omnidirectional communication ranges. The authors also showed that DIV-RANGE and DIV-BER reduce the probability of link failures due to mobility and channel degradation, respectively. The authors in [29] presented a centralized MAC protocol for ad hoc networks with MIMO links, namely stream-controlled medium access (SCMA), which exploits the key optimization considerations of MIMO systems (e.g., coloring, fair allocation, stream control). The authors then extended the SCMA protocol to be distributed. The results showed that the distributed SCMA protocol approximates the centralized one. The application of MIMO techniques in mobile ad hoc networks (MANETs) was explored in [30]. The authors focused on MANETs in which the spatial diversity technique is used to combat fading and achieve robustness in the presence of user mobility. They also developed analytical methods to characterize the saturation throughput for MIMO-based multi-hop networks.

The author in [31] studied the MIMO diversity-multiplexing tradeoff for ad hoc networks. Specifically, two asynchronous cooperative diversity schemes were proposed, namely distributed delay diversity and asynchronous space-time coded cooperative diversity schemes. The author showed that in terms of the overall diversity-multiplexing tradeoff, the proposed independent coding based distributed delay diversity and asynchronous space-time coded cooperative diversity schemes achieve the same performance as the synchronous space-time coded approach. Note that the later scheme requires an accurate symbol-level timing synchronization to ensure signals arriving at the destination from different relay nodes are perfectly synchronized. A spectrally efficient strategy was proposed in [32] for cooperative multiple access (CMA) channels in ad hoc networks with multiple users. According to this strategy, each user transmits a mixture containing its own information as well as the other users information (by applying superposition coding), which means that each user shares parts of its power with the others. It was shown that since the proposed CMA system can be seen as a precoded point-to-point multiple-antenna system, its performance can be best evaluated using the diversity-multiplexing tradeoff. By categorizing the outage events, the diversity-multiplexing tradeoff can be obtained. The authors in [33] studied the diversity-multiplexing tradeoff for multi-access relay channel (MARC) with static and flat fading. The authors developed two strategies, namely multi-access amplify-and-forward (MAF) and multi-access decode-and-forward

(MDF), which help the users gain the benefit of cooperative diversity without changes in their devices. The results in [33] suggested that in the regime of light system loads, both strategies offer improved performance to each user as if no other users interfere or contend for the relay. In the regime of heavy loads, the MARC with MAF was shown to offer better performance. Moreover, the MAF protocol was shown to be optimal in the regime of high multiplexing.

In this paper, we investigate the feasibility of adapting the antenna configuration in a MIMO-based wireless packet network, where each node has two antennas that it can configure to achieve diversity or multiplexing gains. Each link can effectively operate in one of five possible modes: 1×1 (SISO), 2×1 (MISO-D), 1×2 (SIMO-D), 2×2 (MIMO-D), and 2×2 (MIMO-M), where the second, third, and fourth configurations provide diversity (D) gain, whereas the last configuration provides multiplexing (M) gain. We propose a power-controlled protocol, called combined MAC (CMAC), in which the antenna mode, the transmission power, and the modulation order are jointly adapted on a per-packet basis such that a throughput- and energy-dependent utility function is maximized. We conduct a joint optimization to control the tradeoff between energy consumption and network throughput. In contrast to our previously proposed E-BASIC protocol [34] (which exploits MIMO's diversity gain only), CMAC offers the following additional features. First, CMAC exploits both diversity and multiplexing gains. Second, CMAC accounts for both the energy consumption and the throughput, and achieves an "optimal" tradeoff between the two. Third, CMAC allows for concurrent transmissions to take place in the vicinity of a receiving terminal, which is not the case for E-BASIC (the control packets in E-BASIC are used to *silence* potentially interfering terminals). Fourth, in contrast to E-BASIC which uses a fixed modulation scheme, CMAC also adapts the modulation order.

The rest of the paper is organized as follows. We present CMAC in Section 2. In Section 3, we discuss the computation of various power-related parameters. The performance of CMAC is studied via simulations in Section 4, and is contrasted with three reference protocols (IEEE 802.11, POWMAC, and MIMO-POWMAC). Section 5 summarizes our main findings.

2 The CMAC protocol

CMAC is a MIMO-adaptive power-controlled MAC protocol that aims at maximizing a utility function that depends on both energy consumption and throughput. It allows multiple interference-limited transmissions to take place in the vicinity of a receiving terminal. The channel access process (described in Fig. 1) is inspired by the SISO-based POWMAC [10]. Specifically, the protocol uses a modified CSMA/CA approach, whereby nodes use control packets to contend for the channel prior to transmitting their data packets concurrently. The contention period, called the access window (AW), consists of a *variable number* of fixed-duration access slots. Each access slot (AS) consists of the durations of three fixed-length control packets plus a maximum (known) backoff interval $\kappa_{\max}$. An access slot allows a pair of terminals to agree on the appropriate setting of their transmission parameters (i.e., antenna mode, transmission power, modulation order) and inform other nodes of these values.

Depending on the location of the AS within the AW, terminals are classified into *master* and *slave terminals*. More specifically, a master terminal is a terminal that succeeds in acquiring the first AS in the AW. Such a terminal has a packet to transmit and is not aware of any *scheduled* activity (transmission/reception) in its vicinity. For example, terminal A in Fig. 1 is a master terminal. It initializes a new AW, and sets its size in

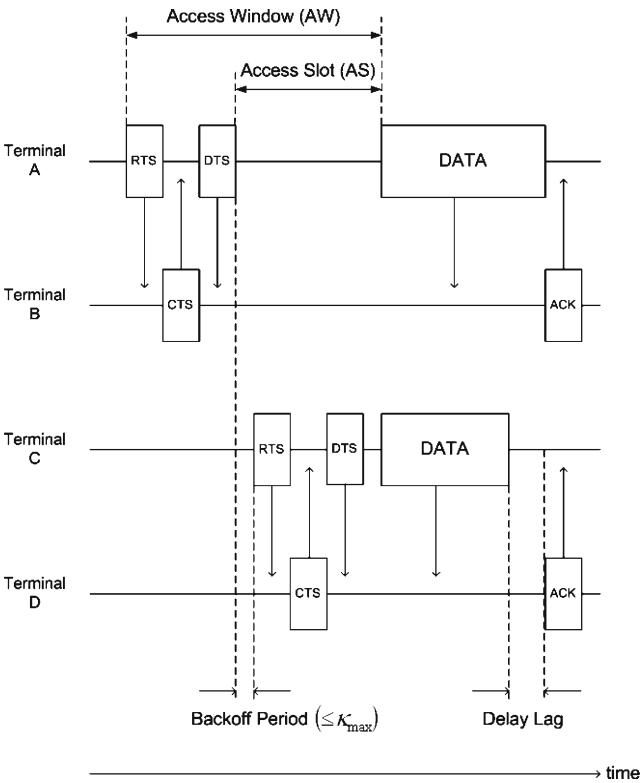

Figure 1 Example that illustrates the channel access mechanism in CMAC

access slots (denoted by $N_{AW}^{(A)}$) according to a load- and collision-dependent algorithm that is described in [10]. The objective of such an algorithm is to maximize the number of successful concurrent transmissions through an incremental adjustment (increase or decrease) of the AW size. Note that while all terminals independently and continuously execute this algorithm, a terminal starts using its computed $N_{AW}^{(.)}$ value only when it acts as a master. In Fig. 1, $N_{AW}^{(A)} = 2$. The master terminal announces its $N_{AW}^{(.)}$ in its first control packet.

2.1 Channel access for a master terminal

Consider the situation at terminal A that has data to transmit to terminal B. According to the IEEE 802.11 standard, there are two cases for terminal A. First, if the medium is sensed idle *for the first time* for a distributed inter-frame space (DIFS) duration, A directly starts transmitting its RTS. Second, if the medium is sensed busy, A starts by randomly selecting a backoff duration $\kappa \sim \text{uniform}\{0, \kappa_{\max}\}$. A counter of value κ is then set (in practice, κ is expressed as a whole number of an appropriately selected time unit). The rationale behind this design is to decrease the chances of collisions between control packets (i.e., RTS/CTS). This reduction in collisions results in a decrease in the number of packet retransmissions, and therefore reduces the total energy consumption for a communication (which includes the energy required for transmission, retransmissions, etc.). As in the classic CSMA/CA approach, terminal A senses the channel periodically. It decrements the counter whenever the channel is sensed idle. Once the counter value reaches zero and the channel is idle, terminal A accesses the channel. It initiates a new AW, i.e., it becomes a master terminal, by sending an RTS packet at a fixed power $P_{\max}$ using the MIMO-D mode, ensuring the farthest transmission range for this packet. The RTS packet includes the value of $N_{AW}^{(A)}$ as well as the value of the maximum allowable power that terminal A can use without disturbing any of its neighbors, denoted by $P_{MAP}^{(A)}$. For a master terminal, this latter parameter is equal to $P_{\max}$. Note that the negative impact of sending the RTS at the maximum power is significantly reduced in CMAC, as the protocol allows for concurrent data transmissions to occur. In fact, CMAC increases the spatial reuse compared to IEEE 802.11, and the impact of the RTS power on the spatial reuse in CMAC is much less than that in IEEE 802.11. The CTS and DTS packets in CMAC are transmitted to only those terminals that can actually make use of the collision avoidance information. This has the added advantage of reduced contention among control packets, leading to an increase in the spatial reuse.

Upon receiving the RTS packet, terminal B computes the "optimal" antenna mode, the transmission power (P_{AB}), and the optimal modulation order (b^*) for the ensuing data packet from A to B. Such computation requires the channel gain from A to B, which terminal B determines from $P_{\max}$ and the received power of the RTS packet. Optimization is done by maximizing the following utility function:

$$u = (1 - \alpha)(1/E) + \alpha T \tag{1}$$

subject to a constraint on the transmission power. In Eq. 1, E is the *minimum* required energy for the upcoming data transmission at the given antenna mode, T is the throughput of that transmission, and α is a parameter that controls the tradeoff between energy and throughput ($0 \leq \alpha \leq 1$). For a given packet, the u value is computed for each antenna mode. The combination of E and T that maximizes u is then used in the upcoming transmission.

It should be noted that in this paper we conduct a joint optimization to control the tradeoff between E and T. Therefore, our goal is to come up with an expression that relates E and T. We relate them via α, so that according to the target application, one can choose α to give more weight to either quantity. Although E and T may seem unrelated, a closer look at them indicates that they are actually mutually dependent, i.e., a higher T comes at the cost of a higher E, and vice versa. Note that several possibilities exist for choosing u. For example, we can maximize $u = T/E$, or minimize E subject to a constraint on T, etc. We chose the expression in Eq. 1 for several reasons. First, we needed a utility function that involves a parameter that controls the tradeoff between E and T. This way, one can support a variety of applications with different degrees of significance for energy/throughput. Second, the utility function in Eq. 1 ensures fairness between E and T. This is due to the fact that $0 \leq \alpha \leq 1$, and that both E and T can get the same value of preference, i.e., E gets a weight of $1 - \alpha$ and T gets the complimentary part of it.

When deciding the antenna mode to be used for transmitting a data packet, the value of α for that transmission is not randomly selected. Instead, the range [0,1] is discretized using Δ increments ($\Delta = 0.1$ in our simulations), and the discretized value of α that maximizes u is selected for that transmission. It should be noted that The function u is maximized at either $\alpha = 0$ or $\alpha = 1$. In fact, in the simulations, when discretizing the range [0,1] to search for the optimal

value of α, only two values of α (0 and 1) were observed. Note, however, that the optimal value of α (0 or 1) varies from one packet to another. For example, when the required energy for various modes is high (i.e., transmitter-receiver separation is large), it makes sense to maximize T, i.e., the optimal α is 1. On the other hand, when the required energy is small, $1/E$ is maximized, i.e., the optimal α is 0. Accordingly, CMAC is still a protocol that combines the two types of MIMO gains in the same network, where some links in the network use diversity gain (via SIMO-D, MISO-D, and MIMO-D), whereas other links use multiplexing gain (via MIMO-M). Therefore, CMAC still serves as a combined energy/throughput protocol.

The energy consumption E includes the RF transmission energy as well as the circuit energy at both ends of the link. In turn, the transmission energy depends on the antenna mode through the SNR threshold (γ), which itself varies with the modulation order (b) [13]. For a transmission from A to B, E_{AB} is given by:

$$E_{AB} = \frac{P_{AB} + P_{circuit}}{R} \tag{2}$$

where R is the transmission rate, P_{AB} is the transmission power from A to B that is given by Eq. 11, and $P_{circuit}$ is the circuit power that depends on the antenna mode (it scales linearly with the number of antennas). This $P_{circuit}$ is given by [14]:

$$P_{circuit} \approx M_t\left(P_{DAC} + P_{mix} + P_{filt}\right) + 2P_{syn} + M_r\left(P_{LNA} + P_{mix} + P_{IFA} + P_{filr} + P_{ADC}\right) \tag{3}$$

where P_{DAC}, P_{mix}, P_{LNA}, P_{IFA}, P_{filt}, P_{filr}, P_{ADC}, and P_{syn} are the power consumption values for the digital-to-analog converter, the mixer, the low noise amplifier, the intermediate frequency amplifier, the active filters at the transmitter and the receiver sides, the analog-to-digital converter, and the frequency synthesizer, respectively.

We now show how a complete expression of E as a function of the optimization parameters (antenna mode, P_{AB}, and b) can be obtained based on Eqs. 2, 3, and 11. Note that we do not provide such an expression due to its size. The three components of E are: P_{AB}, $P_{circuit}$, and R. The expression of P_{AB} is given in Eq. 11, which mainly depends on γ. This γ is function of the antenna mode and modulation order. The second component ($P_{circuit}$) is expressed in Eq. 3, which depends on the antenna mode. The third component is R, which is a function of b. Substituting Eqs. 3 and 11 into Eq. 2 results in an expression for E that depends on the antenna mode, P_{AB}, and b.

The second component of u is T, which basically depends on R (which in turn depends on b) and the antenna mode. Note that the achieved T per link for MIMO-M is twice that of the other antenna modes, as MIMO-M allows two independent streams to be transmitted over the two antennas. As a result, T can be expressed as: $T = 2R$ (bits/s) for MIMO-M mode, and $T = R$ (bits/s) for all other modes. In units of packets/s, $T = 2R/S$ (for the MIMO-M mode), where S is the packet size (bits/packet), and $T = R/S$ (for all other modes).

For systems that support adaptive modulation, terminal B can also optimize the modulation order b. Note that b impacts the energy consumption through γ, which depends on the target BER, the specific antenna mode, and the transmission rate (R). In principle, a higher value of b necessitates a higher γ, i.e., more transmission power is required. However, it also means a higher R, i.e., lower transmission time, which in turn reduces the energy consumption. The confluence of the two effects determines the optimal modulation order (b^*). As shown in Fig. 2, b^* generally decreases with the transmitter-receiver distance. The value of b represents the number of bits per symbol. The number of symbols is given by: $M = 2^b$. Therefore, it should be noted that b is the exponent (to the base 2) that determines the order of the used modulation scheme, e.g.,

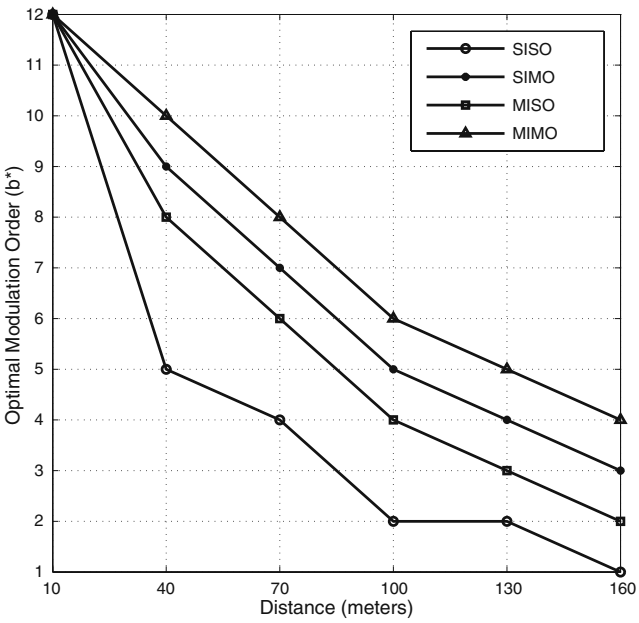

Figure 2 Optimal modulation order (b^*) vs. transmitter-receiver distance for various (fixed) antenna configurations (BER=0.001, $n = 4$, γ values are given in Fig. 4)

$b = 1$ for binary-phase-shift keying (BPSK), $b = 2$ for quadrature-phase-shift keying (QPSK), etc. In principle, the value of b is any positive integer number.

The value of b^* is obtained as follows: for each antenna mode, u is computed which depends on both E and T. The term E includes transmission and circuit energies, where the transmission energy is function of γ. One of the main factors that affect the value of γ is b. The value of b that maximizes u among all its possible values for a specific antenna mode is determined and compared with that of other antenna modes. The one that maximizes u among the five antenna modes is then selected as b^*, which is used in the upcoming transmission.

The γ values for various antenna modes and modulation orders are shown in Fig. 4. For a given antenna mode, γ increases with b. These values of γ were numerically obtained using the expressions in [14]. In [14], the authors provide the average BER ($\bar{P}_b$) as a function of γ for different antenna modes and b values. Specifically, the values of γ were found by evaluating $\bar{P}_b$ over 10000 randomly generated channel samples according to the following equation:

$$\bar{P}_b = E_H \left[\frac{4}{b} \left(1 - \frac{1}{2^{(\frac{b}{2})}} \right) Q \left(\sqrt{\frac{3b\theta(b)}{2^b - 1}} \right) \right] \tag{4}$$

where Q denotes the Q function, H is a scalar fading matrix, in which each entry is a zero mean circularly symmetric complex Gaussian (ZMCSCG) random variable with unit variance (please refer to [14] for more details), and $\theta(b)$ is the instantaneous received SNR, which is given by [14]:

$$\theta(b) = \frac{\|H\|^2}{M_t M_r} \gamma(b) \tag{5}$$

The $\gamma(b)$ values for various antenna modes and modulation orders that yield the desired $\bar{P}_b$ were then obtained.

In Section 3, we discuss how terminal B determines the appropriate power P_{AB} that maximizes the function u. If the computed P_{AB} is greater than the minimum transmission power required to achieve the target BER ($P_{\min}^{(AB)}$) and less than $P_{\max}$, terminal B responds to A with a CTS packet that is sent at a controlled power level $P_{CTS}^{(B)}$. The value of $P_{CTS}^{(B)}$ is discussed in Section 3. The CTS packet contains the optimal antenna mode, the transmission power P_{AB}, and the modulation order b^* to be used by terminal A. It also contains the master's AW size $N_{AW}^{(A)}$. Further, the CTS contains $P_{MTI}^{(B)}$, which is the *maximum tolerable interference* (MTI) that terminal B can allow *from one future transmission* during B's upcoming data reception. Essentially, $P_{MTI}^{(B)}$ is the load margin per interferer at terminal B *during* the upcoming data reception. The quantity $P_{MTI}^{(B)}$, whose computation is discussed in Section 3, allows other terminals to determine whether or not their interfering transmissions can be tolerated by terminal B. If $P_{AB} < P_{\min}^{(AB)}$, B responds with a negative CTS (NCTS) packet, indicating the infeasibility of the proposed transmission.

Upon receiving B's CTS packet, A sends another control packet, called decide-to-send (DTS), at an adjustable power level. The DTS is used to inform the neighbors of A of the power P_{AB} (note that some of A's neighbors may not have heard B's CTS). A neighbor of A, say terminal C, uses P_{AB} along with the channel gain between itself and terminal A to calculate the expected interference that will come from the $A \rightarrow B$ transmission. This helps the neighbor determine whether or not it can transmit concurrently with A. The DTS packet contains $P_{MTI}^{(A)}$, which in this case refers to the maximum additional interference that A can tolerate from one interferer during the ACK reception.

According to CMAC, A does not need to account for transmissions that have not been scheduled yet. Rather, the future transmissions need to account for A's impact on them as well as their impact on already scheduled transmissions, as explained above.

Note that in the classic CSMA/CA, a carrier sensing mechanism is used so that if A's neighbors do not sense a carrier shortly after hearing the RTS, they assume that the RTS/CTS exchange was not successful. In contrast, CMAC does not use this process, as the transmission power of the data packet (P_{AB}) is typically less than the RTS power ($P_{\max}$), i.e., the carrier sense range for the data packet is smaller than that of the RTS packet.

After the RTS/CTS/DTS exchange is completed, A transmits its data packet to B using the specified parameters. If the transmission is successful, B responds with an ACK packet that is sent using the same antenna mode, transmission power, and modulation order as the data packet. Similar to POWMAC, CMAC protects the reception of the ACK packet through a combination of power control and by delaying the ACK transmission (see [10] for details).

2.2 Channel access for a slave terminal

A slave terminal is any terminal that has a packet to transmit and that is aware of an ongoing AW in its neighborhood. Such a terminal cannot initiate a new AW, but must follow the AW schedule set by a master

terminal, i.e., it can contend during any available slot in the ongoing AW other than the first slot. If the slave terminal misses the ongoing AW (possibly, due to a collision with another terminal that contended during the same slot), it must wait until the scheduled data transmissions are completed before it can access the channel as part of another AW. It should be noted that the designation of master and slave terminals is dynamic, i.e., it varies depending on the access times of various terminals. So a terminal may be a master for a given packet transmission and later becomes a slave for another transmission.

If a slave terminal wishes to contend for the channel, it follows a similar process to that of a master terminal (i.e., random backoff followed by RTS, CTS, and DTS), with a few differences. There is a backoff for any slave terminal from the start of an AS until the RTS of that slave is sent (please see Fig. 1). However, for master terminals, once the master terminal's NAV (network allocation vector) reaches zero and the channel is idle, the master can immediately start its RTS (i.e., it does not back off like slave terminals), and by doing so it actually defines a new AW. Note that the RTS and CTS packets of the slave terminals include the *remaining* number of access slots (including the current slot) in the AW. So in the example of Fig. 1, the RTS from slave terminal C and the CTS from terminal D announce a value of $N_{AW}^{(A)} = 1$. This way, other terminals learn that no more slots are available in the current AW. For slave terminal C, the maximum allowable power that is announced in the RTS is set as follows [10]:

$$P_{MAP}^{(C)} = \min_{u \in \Psi(C)} [\pi_C(u)] \tag{6}$$

where $\Psi(C)$ is the set of terminals in C's vicinity whose scheduled data/ACK receptions overlap in time with C's upcoming data transmission (terminal C determines such overlaps from the durations of the scheduled data/ACK packets that are conveyed in the RTS/CTS/DTS packets) and $\pi_C(u)$ is the maximum transmission power that terminal C can use without disturbing terminal u's scheduled reception. As in [10], $\pi_C(u)$ is given by:

$$\pi_C(u) = \min \left[\frac{P_{MTI}^{(u)}}{G_{Cu}} \right] \tag{7}$$

where $0 < G_{Cu} < 1$ is the channel gain between terminals C and u (determined at terminal C from the transmission and reception power values of overheard control packet(s) coming from terminal u), and $P_{MTI}^{(u)}$ is the MTI at terminal u during u's upcoming data or ACK reception. We later discuss how $P_{MTI}^{(u)}$ is determined.

Upon receiving C's RTS, terminal D computes the parameters for the prospective $C \rightarrow D$ data transmission and responds back with a CTS or an NCTS. For the transmission to go forward, the computed transmission power P_{CD} must be larger than $P_{\min}^{(CD)}$ and smaller than $\min\{P_{\max}, P_{MAP}^{(C)}\}$. If a CTS is received, terminal C proceeds with a DTS, whose format is similar to the one described in the previous section. The transmission of the CTS/DTS packets confirms that a data transmission from C to D will commence with the $A \rightarrow B$ data transmission (the two data transmissions need not be completed at the same time; see [10] for details).

In determining its transmission parameters, a prospective slave terminal must satisfy two *feasibility conditions*. First, the data or ACK transmission from this slave terminal should not affect already scheduled receptions in its neighborhood. Second, the interference caused by already scheduled transmissions should not affect the data or ACK reception of the slave terminal in a way that increases the load factor (we later discuss how the load factor is determined) at that terminal beyond its maximum load factor. The likelihood of satisfying these two conditions can be enhanced by allowing a delay lag between the reception of the last bit of the data packet and the transmission of the corresponding ACK. This is illustrated in Fig. 1, where terminal D waits for $\tau_{ACK}^{(CD)}$ before sending the ACK packet to terminal C. The reason behind this design is to protect the ACK reception at C and also prevent terminal D from causing harmful interference onto other scheduled data/ACK receptions. A delay lag makes it more likely to satisfy both goals without having to change the transmission time of the data packet or the transmission power of the ACK packet (which is set to P_{CD}, as explained before).

To conclude this section, we briefly explain the NAV setting in CMAC. There are two cases to consider. First, if the node's transmission cannot concurrently proceed with another node's transmission, the NAV is set as in IEEE 802.11, i.e., the node has to defer its transmission until the other node's transmission is over. Second, if the node's transmission can concurrently proceed with another node's transmission, the node does not wait for a NAV, as both transmissions can take place simultaneously.

3 Power computations

In this section, we discuss the computations associated with various power parameters in CMAC. Such computations follow similar guidelines to those of POWMAC,

with appropriate extensions to accommodate per-packet adaptation of the antenna mode and modulation order. For illustration purposes, we consider the $A \rightarrow B$ transmission in Fig. 1.

When terminal B receives the RTS packet, it computes the minimum required power for the $A \rightarrow B$ transmission ($P_{\min}^{(AB)}$), which is then used as a basis for determining whether or not the $A \rightarrow B$ transmission should go forward. This power is given by:

$$P_{\min}^{(AB)} = \frac{\gamma \left(P_{thermal} + P_{MAI}^{(B)} \right)}{G_{AB}} = \frac{\gamma \xi^{(B)} P_{thermal}}{G_{AB}} \tag{8}$$

$$= \frac{\gamma \xi^{(B)} P_{thermal} d_{AB}^{n}}{k} \tag{9}$$

where $P_{thermal}$ is the thermal power, $P_{MAI}^{(B)}$ is the measured multi-access interference (MAI) at B, $G_{AB} = \frac{k}{d_{AB}^{n}}$ is the channel gain between terminals A and B, d_{AB} is the distance between A and B, k is an antenna-dependent constant, n is the path-loss factor, and $\xi^{(B)} \stackrel{\text{def}}{=} (P_{thermal} + P_{MAI}^{(B)})/P_{thermal}$ is the load factor at terminal B. This $\xi^{(B)}$ is a measure of the *current* transmission activity in B's neighborhood. Setting P_{AB} to $P_{\min}^{(AB)}$ ensures the minimum energy consumption for the $A \rightarrow B$ transmission, but it does not allow for any additional interference from other (not yet scheduled) transmissions to take place. Hence, to accommodate additional interference from to-be-scheduled transmissions (in this case, the $C \rightarrow D$ transmission), terminal B must choose a higher value for P_{AB}. This is done by replacing $\xi^{(B)}$ in Eq. 9 by $\tilde{\xi}^{(B)}$, the maximum load factor at terminal B. The setting of $\tilde{\xi}^{(B)}$ strongly depends on the energy/throughput tradeoff factor α. Specifically, if $\alpha = 0$, the utility function reduces to an energy-oriented function, so $\tilde{\xi}^{(B)}$ should be set to $\xi^{(B)}$. On the other hand, if $\alpha = 1$, the utility function becomes throughput oriented, and $\tilde{\xi}^{(B)}$ can be chosen as in [10] (other possible settings can also be made). In [10], $\tilde{\xi}^{(B)}$ was selected such that the expected per-bit energy consumption is the same for the IEEE 802.11 scheme (standard CSMA/CA) and the POWMAC protocol, which resulted in $\tilde{\xi}^{(B)} = n + 1$. Accordingly, for CMAC, we take $\tilde{\xi}^{(B)}$ as:

$$\tilde{\xi}^{(B)} = \xi^{(B)} + \left[(n+1) - \xi^{(B)} \right] \alpha. \tag{10}$$

Terminal B then sets P_{AB} (used for both the data and ACK packets) to:

$$P_{AB} = \frac{\gamma \tilde{\xi}^{(B)} P_{thermal}}{G_{AB}} = \frac{\gamma \left(\xi^{(B)} + \left[(n+1) - \xi^{(B)} \right] \alpha \right) P_{thermal} d_{AB}^{n}}{k}. \tag{11}$$

It should be noted that the main factors that affect the value of P_{AB} are γ (which is a function of the antenna mode and b) and α. Therefore, the transmission mode and b that result in the minimum value of P_{AB} among the five possible modes are used in transmitting a data packet. The value of α should be also examined for all discretized increments of α's range, so that it results in the minimum value of P_{AB} with respect to γ and α. This minimization aims at maximizing the utility function u according to Eq. 1.

If $P_{\min}^{(AB)} < P_{AB} \leq \min \left\{ P_{MAP}^{(A)}, P_{\max} \right\}$, the transmission can go forward. In this case, B needs to calculate $P_{MTI}^{(B)}$. To do this, B first calculates the total additional interference ($P_{MAI-add}^{(B)}$) that B can tolerate from other to-be-scheduled transmissions while still satisfying its SNR threshold γ. This $P_{MAI-add}^{(B)}$ can be expressed as [10]:

$$P_{MAI-add}^{(B)} = \frac{G_{AB} \left(P_{AB} - P_{\min}^{(AB)} \right)}{\gamma} \tag{12}$$

$$= \left(\tilde{\xi}^{(B)} - \xi^{(B)} \right) P_{thermal}. \tag{13}$$

$P_{MAI-add}^{(B)}$ should account for interferers that are within the maximum transmission range of B $\left(P_{MAI-inside}^{(B)} \right)$ as well as those that are outside that range $\left(P_{MAI-outside}^{(B)} \right)$. Out-of-range interference can be estimated by observing the similarity between the role of a receiver in MANETs and that of a base station in cellular systems [10]. Accordingly,

$$P_{MAI-outside}^{(B)} = \beta P_{MAI-inside}^{(B)} \tag{14}$$

where $\beta \approx 0.5$ for the two-ray propagation model and uniformly distributed terminals.

As for $P_{MAI-inside}^{(B)}$, this interference margin should be divided *equally* among all future in-range interfering transmissions that may be scheduled in the remaining slots of the AW (the rationale is that the interference margin is a network commodity that should be distributed fairly among terminals). Accordingly, terminal B sets $P_{MTI}^{(B)}$ as follows:

$$P_{MTI}^{(B)} = \frac{P_{MAI-add}^{(B)}}{(1+\beta) N_{AW}^{(A)}}. \tag{15}$$

If a CTS packet is to be transmitted, its transmission power is set as follows:

$$P_{CTS}^{(B)} = \min \left[\gamma P_{thermal} \frac{\tilde{\xi}^{(B)} P_{\max}}{P_{MTI}^{(B)}}, \tilde{\xi}^{(B)} P_{\max} \right]. \tag{16}$$

The main reason behind transmitting the DTS and CTS packets at a controlled power is that they reach

all and only potentially interfering terminals. This improves the spatial reuse for the control packets themselves and reduces their collisions. To further illustrate, recall that in CMAC, a receiver, say B, sends a CTS packet that contains collision avoidance information, namely $P_{MTI}^{(B)}$, to bound the transmission power of potentially interfering neighbors. A terminal, say C, that hears this packet sets its $P_{MAP}^{(C)}$ according to Eq. 6. If the maximum transmission power in CMAC $\left(\tilde{\xi} P_{\max}\right)$ is less than $P_{MTI}^{(B)}/G_{CB}$, the collision avoidance information is actually irrelevant to terminal C, and the CTS packet has reached farther than necessary. In CMAC, this issue is not harmful as in the IEEE 802.11 scheme, simply because control packets in CMAC do not prevent neighbors from transmitting. Nonetheless, one way that CMAC employs to overcome this issue is to transmit the CTS and DTS packets only to terminals that can actually make use of the collision avoidance information. This has the added advantage of reduced contention among control packets, leading to an increase in the spatial reuse.

It should be noted that an NCTS packet is sent from A to B to prevent multiple RTS retransmissions from A, as A will resend its RTS if it does not get a response from B. The philosophy behind this design is to prevent transmissions from taking place over links that perceive high interference. This consequently increases the number of active links in the network, subject to the available power constraints, and limits the energy consumed in the communication from A to B. Once A receives the NCTS, it backs off for a random duration of time, and then resends its packet. The rationale behind this design is that after backing off, A may be able to transmit its packet to B, as the level of interference may be reduced at the second trial compared to the first one. Rerouting the packet is actually not a preferable choice, as the total delay and overhead increase (since each intermediate node needs to back off and exchange control packets). Moreover, chances of collisions are increased by rerouting, as more nodes are involved in the rerouting process.

We now explain mathematically the condition of sending an NCTS packet. According to the load planning calculations above, sending an NCTS packet happens when the interference value in the vicinity of B is greater than the one allowed by the planned loading. Recall that ξ is the load factor, $\tilde{\xi}$ is the maximum load factor, and n is the path-loss factor. By comparing Eqs. 9 and 11, it is clear that the situation $P_{AB} < P_{\min}^{(AB)}$ occurs when $\tilde{\xi} < \xi$, i.e., when $\left[\xi + [(n+1) - \xi]\alpha\right] < \xi$, which yields to $\xi > n+1$. In our simulations, we use $n = 4$. Therefore, an NCTS is sent when $\xi > 5$.

4 Performance evaluation

We now evaluate the performance of CMAC and compare it with three other protocols: IEEE 802.11, POWMAC, and MIMO-POWMAC [35]. Both IEEE 802.11 and POWMAC use SISO transmissions at a fixed modulation order. The transmission power in IEEE 802.11 is fixed, whereas POWMAC implements TPC to maximize the spatial reuse. MIMO-POWMAC is a MIMO version of POWMAC that provides multiplexing gain but at a fixed modulation order. Note that POWMAC and MIMO-POWMAC are throughput-oriented protocols that aim at maximizing the network throughput regardless of energy consumption.

The four studied protocols achieve the same forward progress per hop, as the maximum transmission range is the same for all of them. Consequently, we can focus on the one-hop throughput. Note that the focus of this paper is on the MAC design and not on the routing design. For this reason, we only simulate single-hop scenarios. It should be noted that it is possible to study the routing effect by using our design in multi-hop ad hoc networks. In this case, there will be implications in terms of topology discovery and routing design, which are beyond the focus of this paper. Notice that when a min-hop routing protocol is used and the maximum transmission range for various protocols is the same (which is the case in our simulations), the routing will have no impact on the relative performance of the various protocols.

It should be noted that in our simulations, we study the interference effect caused by other contention regions. Recall that CMAC allows for multiple concurrent transmissions to take place in the vicinity of a receiver. To study the interference effect of the MAC protocol in a distributed setting of a multi-hop network, we break the multi-hop path into multiple single-hop paths. This way, we do not lose the interference characteristics of the network. By allowing for concurrent transmissions to take place, we allow several links to contend for the channel, which results in multiple overlapping contention regions, as shown in Fig. 3. In this Figure, the dotted circle indicates the transmission range (contention region) of node B (which transmits its data to node A), the solid circle indicates the transmission range (contention region) of node C (which transmits its data to node D), and the dashed circle indicates the transmission range (contention region) of node E (which transmits its data to node F).

Data packets are assumed, for simplicity, to be of equal size. The PSK modulation scheme is used with $b = 1$ for IEEE 802.11, POWMAC, and MIMO-POWMAC, and adaptive b is used for CMAC. A

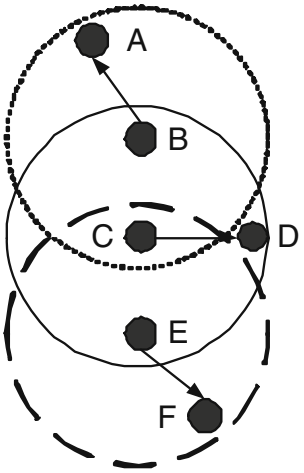

Figure 3 Example that shows multiple overlapping contention regions in CMAC

transmission rate of 1 Mbps is used for the fixed-modulation-scheme protocols. Our setup limits retransmission trials (when collision happens) to 3 for data packets, and 5 for control packets. Other simulation parameters are given in Table 1. Figure 4 shows the SNR values of different antenna modes as a function of b, obtained from [13]. The possible values of b are all integers from 1 to 12. We assume that the buffers have infinite sizes, although in reality the buffers can have finite sizes. However, given that the cost of a memory is cheap, it is realistic to assume that the buffers are large. In this case, the buffer overflow is not necessarily an issue. Our results are based on simulation experiments conducted using CSIM (a C-based process-oriented discrete-event simulation package [36]).

Note that IEEE 802.11, POWMAC, and MIMO-POWMAC do not consider energy saving, whereas

Table 1 System parameters

Data-packet size	2000 bytes
Transmission range	750 meters
Carrier-sense range	1500 meters
Path-loss factor (n)	4
$P_{\max}$	31.6228 mW
$P_{thermal}$	$2.52 * 10^{-14}$ W
$\kappa_{\max}$	80 μs
N_{AW}	5
Control-packets size	20 bytes
BER	0.001
P_{DAC}	15 mW
P_{ADC}	15 mW
P_{mix}	30.3 mW
P_{filt}	2.5 mW
P_{filr}	2.5 mW
P_{syn}	50 mW
P_{LNA}	20 mW
P_{IFA}	2 mW
N_f	10 dB

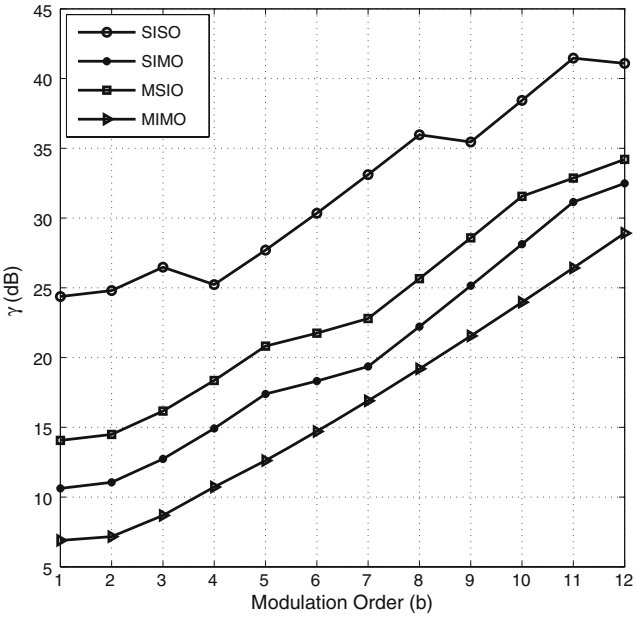

Figure 4 SNR (γ) values for different antenna modes

CMAC takes care of such factor. Therefore, we study the energy and throughput performance (via the first two figures of this section) under an energy-oriented protocol, namely E-BASIC [34]. The reason that we do not consider E-BASIC in all simulation figures is that its performance was extensively studied in our previous work [34]. Note that E-BASIC is expected to improve the energy performance over CMAC, as it exploits MIMO's diversity gain only. On the other hand, E-BASIC is expected to result in worse throughput performance than CMAC, as E-BASIC uses control packets to *silence* potentially interfering terminals (please see Section 1 for more details about E-BASIC). Therefore, we just study E-BASIC for the first two figures to show its energy and throughput performance relative to the other four protocols. Please refer to [34] for more simulation experiments regarding E-BASIC.

4.1 Random-grid topologies

We first study the performance of the four protocols under random-grid topologies. In these topologies, nodes reside in a square area of length 1500 meters. This area is divided into 25 smaller squares, one for each terminal (see Fig. 5). The location of the terminal within a small square is selected randomly. The random waypoint mobility model [37] is used, with a terminal speed that is uniformly distributed in the interval [0,2] meters/second. Each terminal generates packets according to a Poisson process of rate λ packets/s (same for all terminals). The destination terminal is also

selected randomly from the one-hop neighbors. Unless stated otherwise, tradeoff factor α is set to 0.2, and $\lambda = 20$ packets/s.

It should be noted that random-grid topologies are realistic. The random-grid topology models constrained mobility scenarios. For example, a building could have various offices, where each office contains one wireless device (e.g., laptop). Mobility is allowed in that office (the officer can move the laptop), but it is constrained to that office (i.e., the officer cannot move the laptop outside the office). Each such office would map into one of the smaller squares in Fig. 5. The location of a node within each grid is randomly selected, which represents the realistic situation of a laptop within an office.

Figure 6 depicts the average energy consumption per a correctly received packet (E_{avg}) versus λ. It shows that IEEE 802.11 and POWMAC require roughly the same energy, which is expected because the interference margin in both protocols was chosen so that they consume the same energy per bit. The energy consumed by MIMO-POWMAC is almost twice that of POWMAC because of its exploitation of the MIMO multiplexing gain. Recall that the main goal of MIMO-POWMAC is to exploit MIMO's multiplexing gain. Therefore, MIMO-POWMAC is a throughput-oriented protocol that aims at maximizing the network throughput regardless of energy consumption. As a result, it is not expected to give better energy performance than POWMAC. Instead, it improves the throughput performance (as shown in the following figures). CMAC saves a significant amount of energy relative to those protocols. E-BASIC improves the energy performance over CMAC, as it exploits MIMO's diversity gain only.

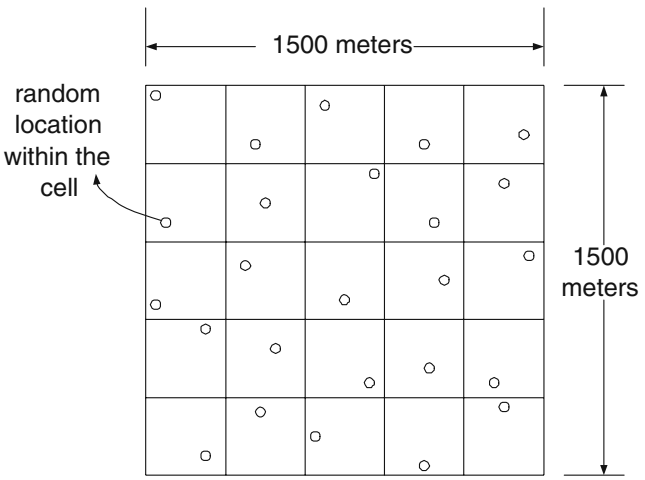

Figure 5 Random-grid topology

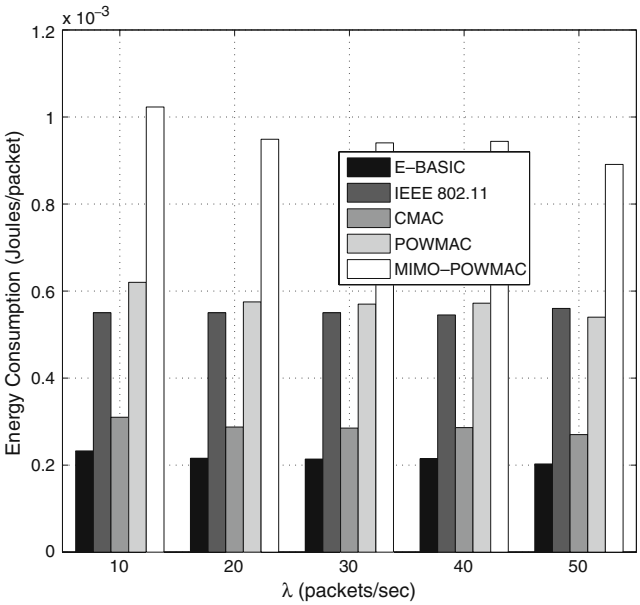

Figure 6 Energy consumption vs. λ (random-grid topologies)

Figure 7 depicts the network throughput versus λ. Note that in this paper, what we refer to as throughput is exactly the goodput, i.e., the total number of correctly-received packets within a duration of time (packets/s). POWMAC achieves higher throughput than IEEE 802.11 due to the increase in the number of simultaneous transmissions. E-BASIC achieves approximately the same throughput performance as IEEE 802.11, as both of them use the control

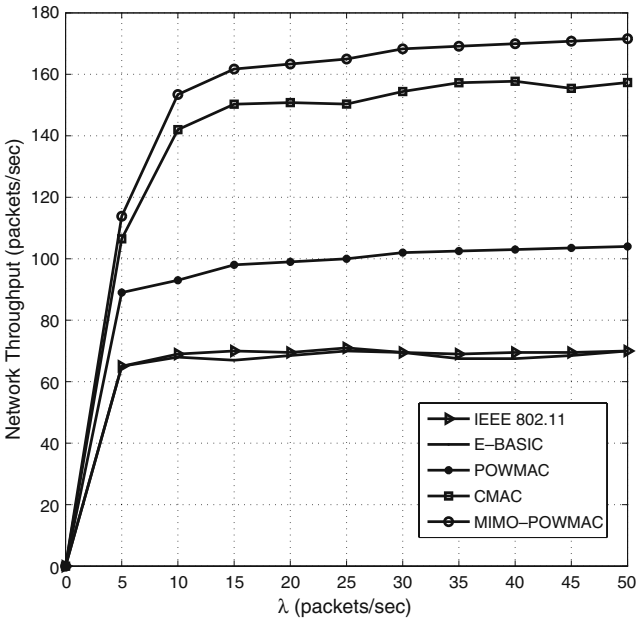

Figure 7 Network throughput vs. λ (random-grid topologies)

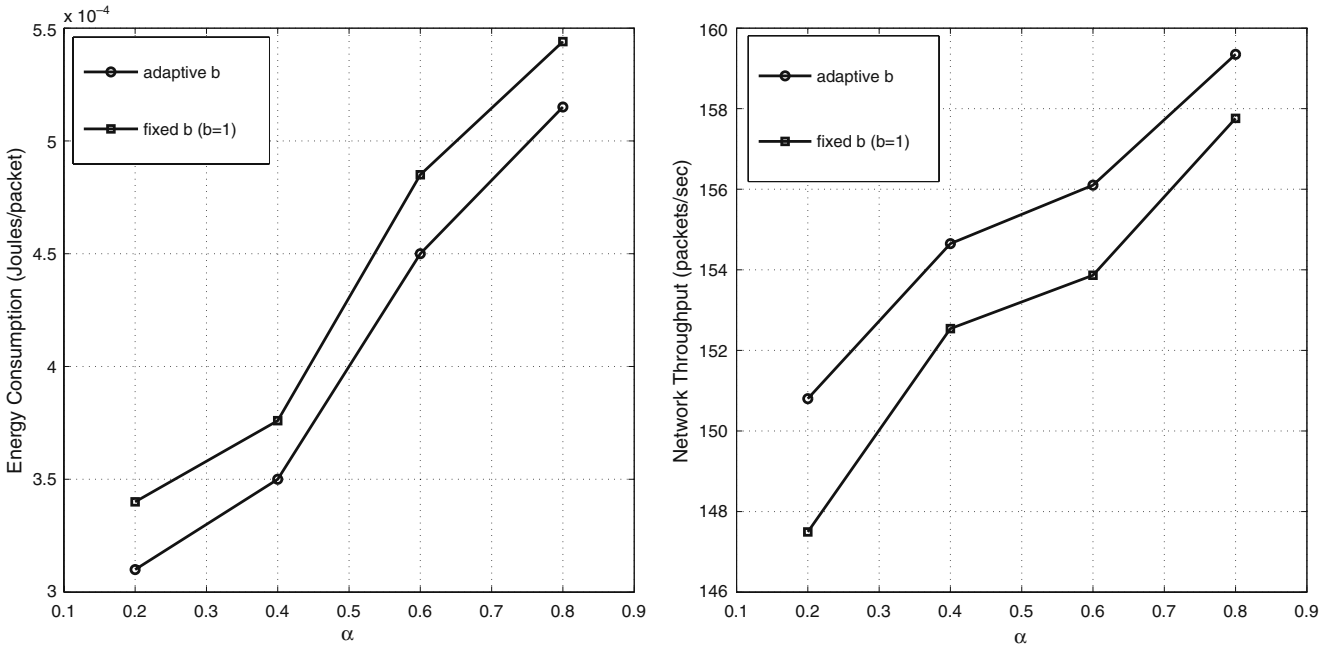

a Energy consumption vs. α. **b** Network throughput vs. α.

Figure 8 Energy and throughput performance vs. α (random-grid topologies) (**a**, **b**)

packets to *silence* potentially interfering terminals. MIMO-POWMAC further improves the throughput of POWMAC through its MIMO multiplexing gain. CMAC achieves better throughput performance than POWMAC, as it adapts the transmission power, the antenna mode, and the modulation order, but its throughput is slightly less than that of MIMO-POWMAC. This is because CMAC accounts for the energy-throughput tradeoff, and not only throughput as MIMO-POWMAC does.

Generally, energy and throughput depend on α and b. The effect of both factors is studied in Fig. 8a and b, respectively. Both figures show that dynamically optimizing b improves the performance compared to the non-adaptive case ($b = 1$). It should also be noted that the lower the α, the better the energy performance, whereas the higher the α, the better the throughput performance, which is in line with Eq. 1.

Figure 9 depicts a histogram for the number of simultaneous transmissions. The figure shows that using the MIMO-M mode in MIMO-POWMAC decreases the number of simultaneous transmissions compared with the SISO mode of POWMAC. This is due to the difference in the required SNR values between the two modes. CMAC has higher likelihood of having one transmission compared to POWMAC and less than that for MIMO-POWMAC, which can be explained from the previous figure. Regarding IEEE 802.11, only one transmission is allowed in a neighborhood at any time.

Figure 10 depicts the network throughput versus the transmission range for the various protocols with $\lambda = 20$ packets/s. CMAC improves the throughput over IEEE 802.11 and POWMAC, whereas MIMO-POWMAC achieves slightly better throughput performance than CMAC, which is in line with the behavior in Fig. 7. Note that in general the throughput increases

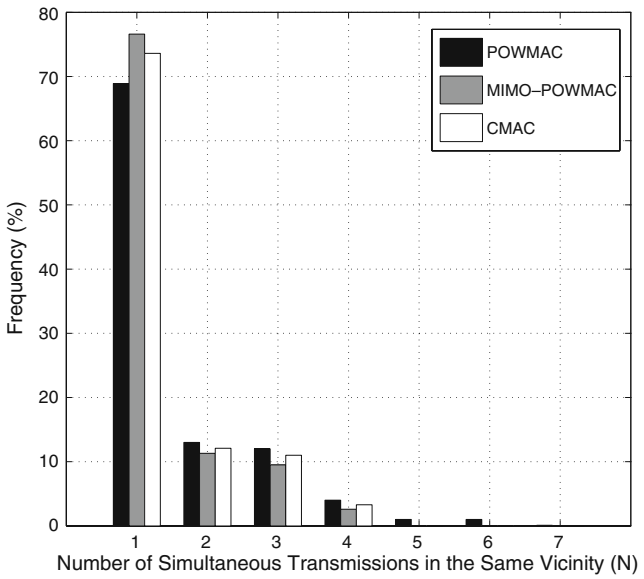

Figure 9 Histogram of simultaneous transmissions (random-grid topologies)

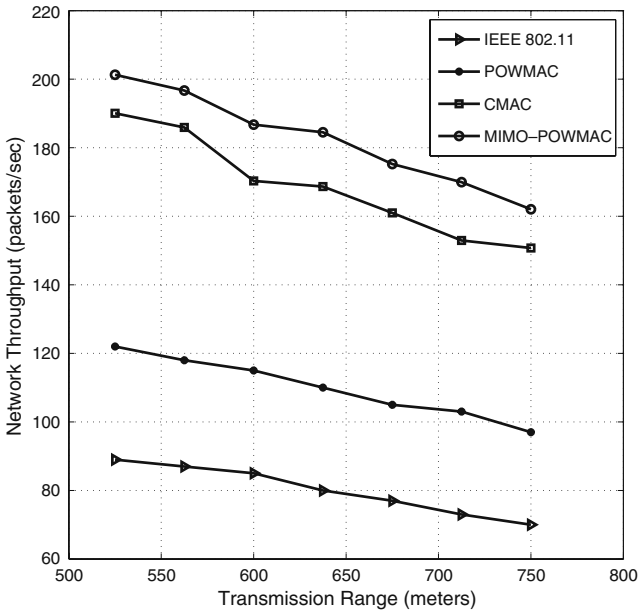

Figure 10 Network throughput vs. transmission range (random-grid topologies)

as the transmission range decreases, as a smaller transmission floor per transmission is reserved at smaller ranges. This allows multiple transmissions to proceed concurrently.

Next, we study the impact of data-packet size on the throughput. We set $\lambda = 20$ packets/s. The throughput is shown in Fig. 11 for different packet sizes. For IEEE 802.11, the throughput slightly increases as the packet size grows. This is because the overhead is fixed for both small and large packets. The improvement in throughput is more magnified for CMAC, POWMAC, and MIMO-POWMAC because of the more significant effect of the contention overhead.

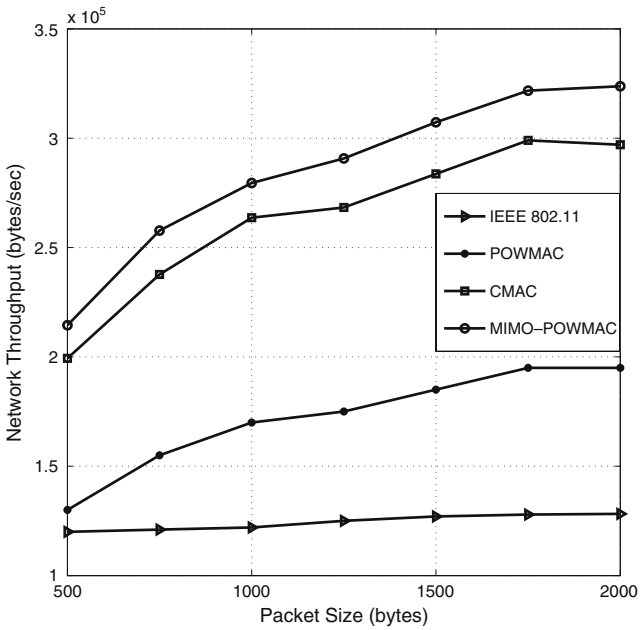

Figure 11 Network throughput vs. data-packet size (random-grid topologies)

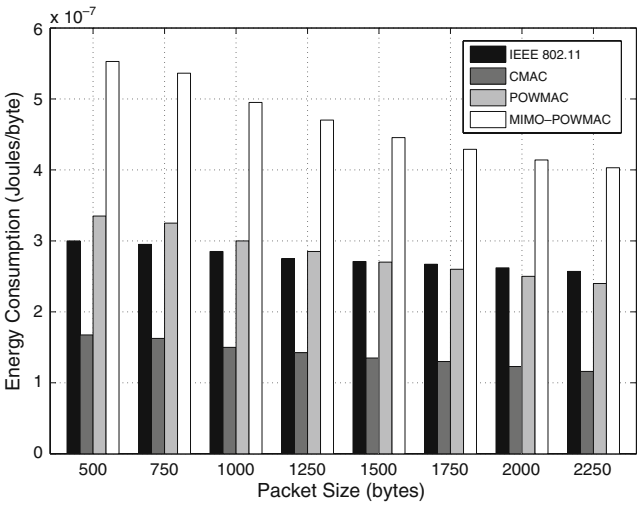

Figure 12 Energy consumption vs. data-packet size (random-grid topologies)

The impact of the data-packet size on the energy performance for the four protocols is studied in Fig. 12. The figure shows that the energy consumption decreases as the packet size increases. The reason is that the fraction of energy consumed on control packets compared to data packets is smaller when data packets are larger.

To conclude this section, we show in Table 2 the percentage of antenna modes used for CMAC under various α values. This table shows that MIMO-D is used more often than the other modes when α is small (e.g., 0.2) due to the fact that under such a small value of α, diversity gain is more preferable than multiplexing gain. Moreover, MIMO-D is more preferable than the other diversity modes according to the transmitter-receiver distance, as MIMO-D achieves less total energy consumption than the other diversity modes when the transmission energy dominates the circuit energy. For

Table 2 Percentage of used antenna modes for random-grid topologies

Antenna mode	$\alpha = 0.2$	$\alpha = 0.4$	$\alpha = 0.6$	$\alpha = 0.8$
MIMO-D	62%	54%	14%	7%
SIMO-D	12%	10%	4%	2%
MISO-D	10%	9%	3%	1%
MIMO-M	9%	21%	77%	89%
SISO	7%	6%	2%	1%

large values of α (e.g., 0.8), MIMO-M is used more often than the other modes, as multiplexing gain becomes more preferable than diversity gain.

4.2 Clustered topologies

In this section, we study the performance under "clustered" topologies. The network has an area of 600 × 600 square meters, in which 16 terminals are split into 4 clusters. The clusters are located at the corners of the network area and each has an area of 100 × 100 square meters. Each source terminal selects its destination from the same cluster with probability $1 - p$, and from a different cluster with probability p. A sketch of a clustered topology is shown in Fig. 13. Unless stated otherwise, tradeoff factor α is set to 0.2, and $\lambda = 20$ packets/s.

A clustered topology is commonly used in situations where wireless devices are spread over multiple buildings. Intra-cluster communications correspond to communications between different devices in the same building. Inter-cluster communications correspond to communications between devices in different buildings. The destination can be either within the same building (which represents a cluster), or it can be in different buildings. To further explain this situation, consider Fig. 13. The big square represents an area that consists of four buildings. Each square that lies at one of the corners of the big square represents a building. The four nodes within each small square represent wireless devices (e.g., laptops), which are randomly located in each building. Each node within a small square (which represents a laptop) has the ability to communicate (with a probability of $1 - p$) with another laptop among the same building, and with other laptops in the other buildings (with a probability of p).

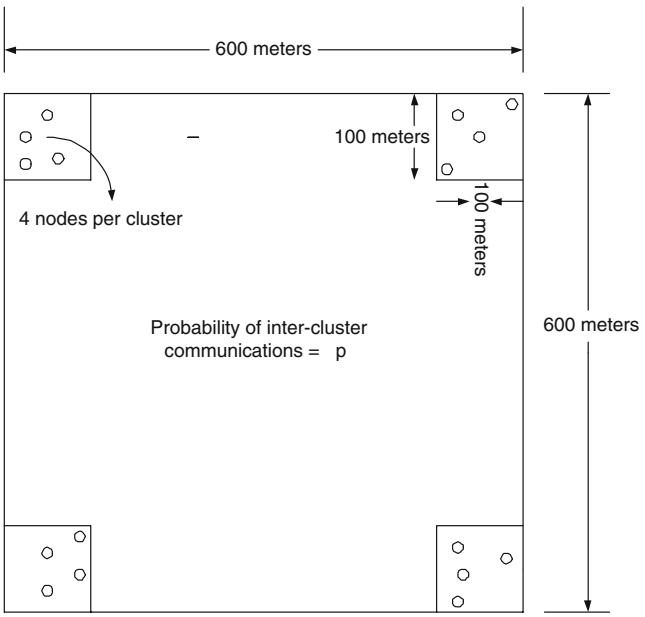

Figure 13 Clustered topology

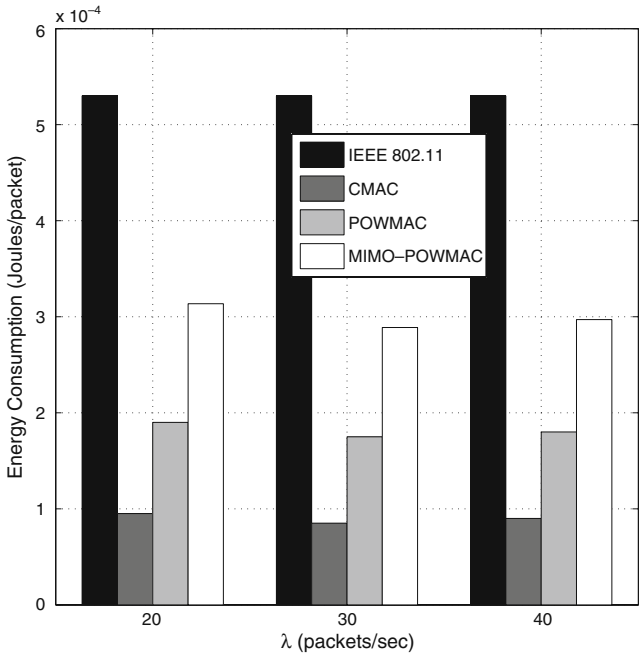

Figure 14 Energy consumption vs. λ under clustered topologies ($p = 0.5$)

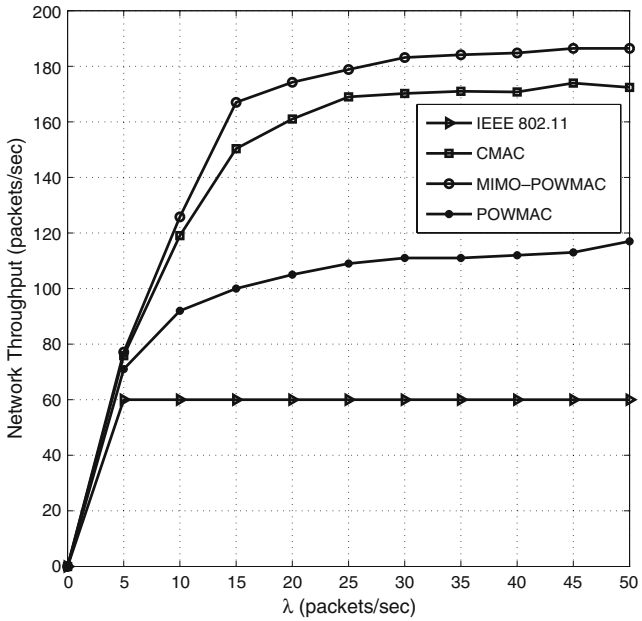

Figure 15 Network throughput vs. λ under clustered topologies ($p = 0.5$)

Figure 14 depicts the total energy consumption versus λ at $p = 0.5$. The figure shows the significant increase in energy consumption that is needed to support the MIMO-M mode for MIMO-POWMAC, which is close to twice that of the SISO mode for POWMAC. CMAC achieves a significant improvement in energy efficiency relative to IEEE 802.11, POWMAC, and MIMO-POWMAC. The same reasons mentioned for Fig. 6 apply here. As in random-grid topologies, the energy and throughput performance depends on α and b. The lower the α, the better the energy performance, whereas the higher the α, the better the throughput performance as shown in Fig. 8a, b, respectively.

Figure 15 depicts the network throughput versus λ at $p = 0.5$. The figure shows that CMAC achieves better throughput performance than IEEE 802.11 and POWMAC, and slightly less than that of MIMO-POWMAC.

Note that for small values of p, a terminal communicates mostly with terminals within its own cluster; thus requiring much less transmission power than $P_{\max}$. We now study the energy and throughput performance under a smaller value of p to highlight the effect of p. Figure 16 compares the energy consumption of CMAC with that of the other protocols at $p = 0.25$. This figure shows that a significant improvement in energy consumption is achieved by CMAC compared to the results of $p = 0.5$ due to the reasons mentioned above.

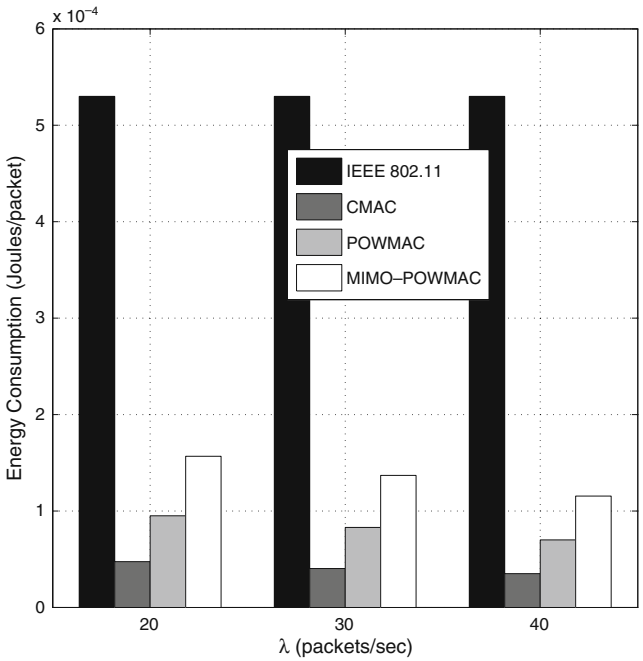

Figure 16 Energy consumption vs. λ under clustered topologies ($p = 0.25$)

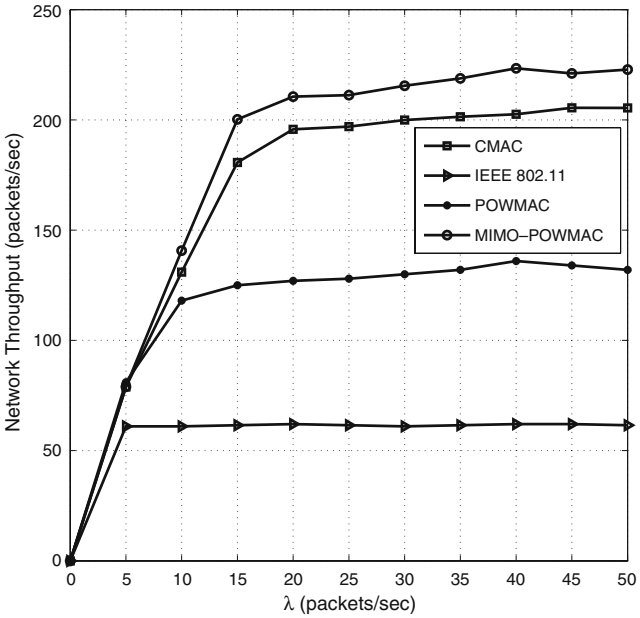

Figure 17 Network throughput vs. λ under clustered topologies ($p = 0.25$)

Note that IEEE 802.11 is the only protocol among the four compared protocols that does not benefit from the locality of the traffic, as all terminals are within the carrier sense range of each other.

The effect of changing the value of p on the throughput is studied in Fig. 17, which depicts the throughput of the four protocols at $p = 0.25$. This figure shows that CMAC achieves better throughput with smaller values of p, as previously discussed.

5 Conclusions

In this paper, we proposed a power-controlled protocol, coined CMAC, for MIMO-capable wireless networks with two antennas per node. CMAC combines diversity and multiplexing gains, and allows for dynamic adaptation of these gains to maximize a utility function that depends on both the energy consumption and throughput. The protocol has the ability to adapt the antenna mode, the transmission power, and the modulation order on a per-packet basis. Generally, energy-oriented optimizations come at the cost of reduced network throughput. In this paper, we accounted for the energy-throughput tradeoff by combining both in one utility function. We studied the performance of CMAC via simulations in two types of ad hoc topologies, and compared it with three other MAC protocols. Simulation results showed that CMAC achieves a significant

improvement in the overall energy consumption and the throughput relative to non-adaptive protocols.

References

1. International Standard ISO/IEC (1999) 8802-11 ANSI/IEEE Std 802.11, 1999 edition. Part 11: Wireless LAN Medium Access Control (MAC) and Physical Layer (PHY) Specifications
2. Gupta P, Kumar PR (2000) The capacity of wireless networks. IEEE Trans Inf Theory 46(2):388–404, March
3. Monks J, Bharghavan V, Hwu W-M (2001) A power controlled multiple access protocol for wireless packet networks. In: Proceedings of the IEEE INFOCOM conference, Anchorage, April 2001, pp 219–228
4. Wu S-L, Tseng Y-C, Sheu J-P (2000) Intelligent medium access for mobile ad hoc networks with busy tones and power control. IEEE J Sel Areas Commun 18(9):1647–1657, September
5. Krunz M, Muqattash A, Lee S-J (2004) Transmission power control in wireless ad hoc networks: challenges, solutions, and open issues. IEEE Netw 18(5):8–14, September
6. Agarwal S, Krishnamurthy S, Katz RH, Dao SK (2001) Distributed power control in ad-hoc wireless networks. In: Proceedings of the IEEE international symposium on personal, indoor, and mobile radio communications (PIMRC), San Diego, September 2001, pp 59–66
7. Gomez J, Campbell AT, Naghshineh M, Bisdikian C (2003) PARO: supporting dynamic power controlled routing in wireless ad hoc networks. ACM/Kluwer J Wirel Netw (WINET) 9(5):443–460, September
8. Jung E-S, Vaidya NH (2002) A power control MAC protocol for ad hoc networks. In: Proceedings of the ACM MobiCom conference, Atlanta, 23–26 September 2002
9. Muqattash A, Krunz M (2004) A distributed transmission power control protocol for mobile ad hoc networks. IEEE Trans Mob Comput 3(2):113–128, April/June
10. Muqattash A, Krunz M (2005) POWMAC: a single-channel power-control protocol for throughput enhancement in wireless ad hoc networks. IEEE J Sel Areas Commun 23(5): 1067–1084 (Special Issue on Advances in Military Wireless Communications), May
11. Xiao Y (2003) A simple and effective priority scheme for IEEE 802.11. IEEE Commun Lett 7(2):70–72, February
12. Xiao Y (2004) An analysis for differentiated services in IEEE 802.11 and IEEE 802.11e wireless LANs. In: Proceedings of the international conference on distributed computing systems (ICDCS), Tokyo, March 2004, pp 32–39
13. Paulraj A, Nabar R, Gore D (2003) Introduction to space-time wireless communications. Cambridge University Press, Cambridge
14. Cui S, Goldsmith AJ, Bahai A (2004) Energy-efficiency of MIMO and cooperative MIMO in sensor networks. IEEE J Sel Areas Commun 22(6):1089–1098, August
15. Cui S, Goldsmith AJ, Bahai A (2005) Energy-constrained modulation optimization. IEEE Trans Wirel Commun 4(5):2349–2360, September
16. Min R, Chadrakasan A (2002) A framework for energy-scalable communication in high-density wireless networks. In: Proceedings of the international symposium on low power electronics and design (ISLPED), Monterey, August 2002, pp 36–41
17. Schurgers C, Aberthorne O, Srivastava MB (2001) Modulation scaling for energy aware communication systems. In: Proceedings of the international symposium on low power electronics and design (ISLPED), Huntington Beach, August 2001, pp 96–99
18. Chen B, Gans MJ (2005) MIMO communications in ad hoc networks. In Proceedings of the IEEE semiannual vehicular technology conference (VTC), May 2005, pp 2434–2438
19. Gilbert JM, Choi W-J, Sun Q (2005) MIMO technology for advanced wireless local area networks. In: Proceedings of the design automation conference (DAC), June 2005, pp 413–415
20. Jafarkhani H, Yousefi'zadeh H, Kazemitabar J (2005) Capacity-based connectivity of MIMO fading ad-hoc networks. In: Proceedings of the IEEE GLOBECOM conference, November 2005, pp 2827–2831
21. Aniba G, Aissa S (2005) Cross-layer design for scheduling and antenna sharing in MIMO networks. In: Proceedings of the IEEE GLOBECOM conference, November 2005, pp 3185–3189
22. Gorokhov A, Gore D, Paulraj A (2003) Receive antenna selection for MIMO spatial multiplexing: theory and algorithms. IEEE Trans Signal Process 51(11):2796–2807, November
23. Tse D, Viswanath P, Zheng L (2004) Diversity-multiplexing tradeoff in multiple-access channels. IEEE Trans Inf Theory 50(9):1859–1874, September
24. Dai L, Sfar S, Letaief K (2005) Towards a better diversity-multiplexing tradeoff in MIMO systems. In: Proceedings of the international conference on communications (ICC), May 2005, pp 2422–2426
25. Sana S, Dai L, Letaief K (2005) Optimal diversity-multiplexing tradeoff with group detection for MIMO systems. IEEE Trans Commun 53(7):1178–1190, July
26. Narasimhan R (2006) Finite-SNR diversity-multiplexing tradeoff for correlated Rayleigh and Rician MIMO channels. IEEE Trans Inf Theory 52(9):3965–3979, September
27. Kountouris M, Francisco R, Gesbert D (2006) Multiuser diversity-multiplexing tradeoff in MIMO broadcast channels with limited feedback. In: Proceedings of IEEE annual asilomar conference on signals, systems, and computers, October 2006
28. Sundaresan K, Sivakumar R (2005) Routing in ad-hoc networks with MIMO links. In: Proceedings of the IEEE international conference on network protocols (ICNP), November 2005, pp 85–98
29. Sundaresan K, Sivakumar R, Ingram MA, Chang T-Y (2004) Medium access control in ad-hoc networks with MIMO links: optimization considerations and algorithms. IEEE Trans Mob Comput 3(4):350–365, October–December
30. Hu M, Zhang J (2004) MIMO ad hoc networks: medium access control, saturation throughput, and optimal hop distance. J Commun Netw 6(4):317–330 (Special Issue on Mobile Ad Hoc Networks), December
31. Wei S (2007) Diversity-multiplexing tradeoff of asynchronous cooperative diversity in wireless networks. IEEE Trans Inf Theory 53(11):4150–4172, November
32. Ratnarajah T, Ding Z, Cowan C (2007) On the diversity-multiplexing tradeoff for wireless cooperative multiple access systems. IEEE Trans Signal Process 55(9):4627–4638, September
33. Chen D, Laneman J (2006) The diversity-multiplexing tradeoff for the multi-access relay channel. In: Proceedings of the conference on information sciences and systems (CISS), March 2006, pp 1324–1328
34. Siam MZ, Krunz M, Muqattash A, Cui S (2006) Adaptive multi-antenna power control in wireless networks.

In: Proceedings of the international wireless communications and mobile computing conference (IWCMC), July 2006, pp 875–880
35. Siam MZ, Krunz M (2007) Throughput-oriented power control in MIMO-based ad hoc networks. In: Proceedings of the IEEE international conference on communications (ICC), June 2007
36. Mesquite Software Incorporation (2006) Mesquite Software homepage. http://www.mesquite.com
37. Broch J, Maltz DA, Johnson DB, Hu Y-C, Jetcheva J (1998) A performance comparison of multi-hop wireless ad hoc network routing protocols. In: Proceedings of the ACM MobiCom conference, October 1998, pp 85–97

Mohammad Z. Siam is a Ph.D. student and a research assistant in the Department of Electrical and Computer Engineering at The University of Arizona, Arizona, USA. He received the B.Sc. and M.Sc. degrees in Electrical Engineering from Jordan University of Science and Technology, Jordan in 2002 and 2004, respectively. His current research interests are in system architecture and communication protocols for wireless networks with emphasis on power control for MIMO-based networks. M. Siam is a member of the IEEE and the ACM.

Marwan Krunz is a professor in the Department of Electrical and Computer Engineering at the University of Arizona and the co-director of Connection One, a joint NSF/state/industry IUCRC cooperative research center. He received the Ph.D. degree in Electrical Engineering from Michigan State University in 1995. From 1995 to 1997 he was a postdoctoral research associate with the Department of Computer Science, University of Maryland, College Park. He also held visiting research positions at INRIA, Sophia Antipolis, France; HP Labs, Palo Alto; and US West Advanced Technologies, Boulder, Colorado. His recent research interests include medium access and routing protocols for mobile ad hoc networks, quality of service provisioning over wireless links, constraint-based routing, WWW traffic modelling, and media streaming. He has published more than 140 journal articles and refereed conference papers in these areas. He received the National Science Foundation CAREER Award (1998–2002). He currently serves on the editorial board for the IEEE/ACM Transactions on Networking and the Computer Communications Journal. He was a guest co-editor for special issues in IEEE Micro and IEEE Communications Magazines. He served as the technical program co-chair for the IEEE INFOCOM 2004 Conference and the 2001 Hot Interconnects Symposium (Stanford University, August 2001). He has served and continues to serve on the executive and technical program committees of several international conferences. He consults for a number of corporations in the telecommunications industry. M. Krunz is a senior member of the IEEE and a member of the ACM.